

MS #71854 v. 3: Astrophysical Journal, 2007, in press

Multiwavelength Monitoring of the Unusual Ultraluminous Supernova SN 1978K in NGC 1313 and the Search for an Associated Gamma-Ray Burst

I. A. Smith

*Department of Physics and Astronomy, Rice University,
6100 South Main MS-108, Houston, TX 77251-1892*

`iansmith@rice.edu`

S. D. Ryder

Anglo-Australian Observatory, PO Box 296, Epping, NSW 1710, Australia

M. Böttcher

*Astrophysical Institute, Department of Physics and Astronomy,
Clippinger Hall 251B, Ohio University, Athens, OH 45701-2979*

S. J. Tingay

*Centre for Astrophysics and Supercomputing,
Swinburne University of Technology, Hawthorn, Victoria, Australia*

A. Stacy

*University of Texas, Department of Astronomy,
1 University Station, C1400, Austin, Texas 78712-0259*

M. Pakull

Observatoire de Strasbourg, 11, rue de l'Université, Strasbourg F-67000, France

and

E. P. Liang

*Department of Physics and Astronomy, Rice University,
6100 South Main MS-108, Houston, TX 77251-1892*

ABSTRACT

We discuss our radio (Australia Telescope Compact Array and Australian Long Baseline Array) and X-ray (*XMM-Newton*) monitoring observations of the unusual ultraluminous supernova SN 1978K in NGC 1313 at ~ 25 years after the explosion. SN 1978K is a rare example of a Type IIn supernova that has remained bright enough to have long-term X-ray and radio observations. The observations probe the dense medium that was ejected by the progenitor star prior to its explosion; the star might have been a Luminous Blue Variable. The radio imaging shows that the source remains compact, but it may be marginally resolved. The radio monitoring shows deviations from a smooth decay suggesting that inhomogeneities are present in the radio emitting region. It appears that a major change occurred in the mass-loss rate of the progenitor star shortly before the supernova event. The X-ray emission between 2000 and 2006 is consistent with the radiation coming from two shocks. All the X-ray data can be fit using the same model (with no systematic evolution or short-term variability) but this has a surprising requirement: the X-ray emitting regions have a very large abundance of helium. This would be consistent with the X-ray emitting shocks being located in a helium-rich layer that was ejected by the progenitor star, or helium-rich material was ejected in the supernova explosion. The unusual properties of the supernova motivated a search for an associated gamma-ray burst (GRB). We show that SN 1978K was inside the $\sim 4\sigma$ error box of GRB 771029. If this association is correct, the GRB was exceptionally underluminous. However, the quality of the gamma-ray burst locations at that time was poor, and this is likely just a chance alignment.

Subject headings: supernovae: individual (SN 1978K) — supernova remnants — galaxies: individual (NGC 1313) — gamma rays: bursts

1. Introduction

The nearby late-type barred spiral galaxy NGC 1313 has long been a subject of detailed multiwavelength observations. It appears to be an isolated galaxy at a distance of only 4.13 Mpc (Méndez et al. 2002). The disk is inclined at 48° to the line of sight (Ryder et al. 1995) permitting an excellent view of the whole galaxy. It has a patchy optical morphology, contains several H I supershells (Ryder et al. 1995), and is rich in young clusters (Larsen 1999). This indicates that it has undergone vigorous irregular star formation.

The diffuse X-ray emission in NGC 1313 is low which has allowed detailed studies of its point sources. Observations have been made by *Einstein*, *ROSAT*, *ASCA*, *XMM-Newton*, *Chandra*, and *Suzaku* (e.g. Fabbiano & Trinchieri 1987; Ryder et al. 1993; Stocke et al. 1995; Colbert et al. 1995; Colbert & Mushotzky 1999; Schlegel et al. 1996, 1999, 2000, 2004; Miller et al. 1998, 2003, 2004; Zampieri et al. 2004; Mizuno et al. 2007; Mucciarelli et al. 2007; Feng & Kaaret 2007).

NGC 1313 contains three ultraluminous X-ray sources (ULXs) that are offset from the center of the galaxy. Two of these – with X-ray luminosities $\gtrsim 10^{40}$ erg/s – have been associated with optical ionized nebulae (Pakull & Mirioni 2002, 2003; Pakull, Gris , & Motch 2006; Liu et al. 2007). Their X-ray spectral and variability properties (with significant changes on time scales as short as 1 day) indicate they contain accreting black holes. Our multiwavelength observations of these two ULXs and the other less luminous persistent and transient X-ray sources in NGC 1313 will be discussed elsewhere (Smith et al. 2007).

The third ULX in NGC 1313 is the unusual luminous supernova SN 1978K. This was the second supernova to be detected and recognized as a supernova from its radio emission and the first from its X-rays (Ryder et al. 1993). There was no X-ray detection by *Einstein* in 1980; the first X-ray detection was by *ROSAT*, 13 years after the explosion. It is rare that supernovae are bright enough to be followed in the X-ray band (Bregman et al. 2003), and SN 1978K is one of only a few that have had long-term monitoring.

There was no evidence for radio emission prior to the supernova. Unlike a “normal” Type II supernova, the peak radio luminosity was very high. SN 1978K is thus one of the most important members of the “Type II_n” sub-class of supernovae (Schlegel et al. 2000).

Observations before the supernova showed the progenitor star to have $B_J \sim 22.1$ in 1974 and 1976, and it was at $B_J \gtrsim 23$ on 1977 October 12, the last observation prior to the explosion (Ryder et al. 1993). The object brightened to $B = 16$ by 1978 July 31, and faded to $B = 18$ by the end of 1978 September (Ryder et al. 1993).

The optical emission lines in SN 1978K are only moderately broad, unlike most supernova ejecta (Ryder et al. 1993; Chugai, Danziger, & Della Valle 1995; Chu et al. 1999). This suggests the surrounding medium was dense, leading to a rapid slowdown of the shock. It is likely that the dense medium is the wind ejected prior to the explosion by the progenitor star, which might have been a Luminous Blue Variable (LBV; Chu et al. 1999; Gruendl et al. 2002).

Hubble Space Telescope observations have shown that the source is still consistent with being point-like (Gruendl et al. 2002). The upper limit of $0.1''$ on the size of the nebula that is currently radiating in the optical (~ 2 pc) is again consistent with the progenitor being

an LBV.

In addition to the moderately broad lines, there are narrow optical emission lines (Chugai, Danziger, & Della Valle 1995; Chu et al. 1999; Gruendl et al. 2002). Some of these likely come from shocked gas in the dense circumstellar wind. Chugai, Danziger, & Della Valle (1995) note the possible presence of the narrow forbidden lines [Fe X] and [Fe XIV] that might originate from hot ($\sim 10^6$ K) shocked gas. Other narrow optical emission lines come from a circumstellar H II region that has not yet been reached by the supernova ejecta and that might result in a re-brightening in the future.

The evolution of the broad-band radio light curves indicated there was a time-independent free-free absorption component required (Montes, Weiler, & Panagia 1997; Schlegel et al. 1999). This is presumably the same H II circumstellar region inferred from the narrow optical lines. This provides further evidence for the suggestion that the progenitor was an LBV.

In this paper, we discuss our radio observations using the Australia Telescope Compact Array (ATCA) and Long Baseline Array (LBA), and X-ray observations using *XMM-Newton* of SN 1978K at ~ 25 years after the explosion. Preliminary results were presented in Smith et al. (2004) and Stacy (2005).

In §2 we show the new radio observations of SN 1978K and discuss the implications for the radio imaging and variability. In §3 we summarize the X-ray monitoring observations from 2000 through 2006 and discuss the modeling of this data. In §4 we describe a search for a gamma-ray burst (GRB) that might have accompanied the supernova. In §5 we conclude with the implications for future observations.

2. Radio Observations

2.1. VLBI Imaging Observations

SN 1978K was observed with an Australian VLBI array consisting of the following antennas: Tidbinbilla 70 m (NASA); ATCA 5×22 m phased array (ATNF); Parkes 64 m (ATNF); Mopra 22 m (ATNF); and Hobart 26 m (University of Tasmania).

A 12 hour observation using all the antennas except Tidbinbilla took place on 2003 February 14 between 00:00 UT and 12:00 UT. This used two 16 MHz bands in the frequency ranges 1.384 – 1.400 GHz and 1.400 – 1.416 GHz. A second 12 hour observation using all the antennas took place on 2003 March 22, also between 00:00 UT and 12:00 UT. This used two 16 MHz bands in the frequency ranges 2.264 – 2.280 GHz and 2.280 – 2.296 GHz.

For both observations the Nyquist sampled, two-bit digitized right circular polarization signals were recorded at each antenna using the S2 tape-based system (Cannon et al. 1997). All the data were correlated at the ATNF S2 correlator (Wilson et al. 1992), and the correlated data were exported to AIPS for standard fringe-fitting and amplitude calibration using measured T_{sys} values from the telescopes. These data were exported to DIFMAP (Shepherd et al. 1994) for further calibration and imaging, using standard self-calibration and clean techniques.

Figure 1 shows the final image from the higher resolution 2.3 GHz data. A single compact component was detected at a signal to noise of ~ 56 (the peak flux density was 28 ± 3 mJy/beam, and the rms image noise 0.5 mJy/beam). The total cleaned flux in this component is 33 ± 3 mJy. The component appears to be marginally resolved. When modeled as a single circular Gaussian component in the (u,v) plane, the best-fit FWHM is 9.5 ± 2.0 mas (c.f. beam dimensions of $29 \text{ mas} \times 12 \text{ mas}$).

At 1.4 GHz the source appears very similar, being marginally resolved and having a best-fit circular Gaussian FWHM of 12 ± 3 mas (c.f. beam dimensions of $38 \text{ mas} \times 17 \text{ mas}$). The estimated sizes at 1.4 GHz and 2.3 GHz are consistent to within their errors. The total flux density of the marginally resolved component at 1.4 GHz is higher than at 2.3 GHz, 56 ± 6 mJy. The source is detected at a signal to noise of ~ 45 (1.4 GHz image rms of 1.0 mJy/beam and peak flux density in the image of 45 ± 5 mJy/beam).

2.2. ATCA Monitoring Observations

Following on from the previous radio observations (Ryder et al. 1993; Montes, Weiler, & Panagia 1997; Schlegel et al. 1999), the ATCA has continued to make occasional observations of SN 1978K. The data acquisition followed the same procedures as outlined in Schlegel et al. (1999). The dataset for each observation and frequency was edited and calibrated using the MIRIAD software package. Rather than estimating the unresolved flux density of SN 1978K from plots of the calibrated visibility amplitude as in Schlegel et al. (1999), the UVFIT task was used instead in the visibility domain to fit a point source at the known location of SN 1978K.

Figure 2 and Table 1 add 7 data points at all four frequencies (8640, 4790, 2496, and 1376 MHz) to the results presented by Schlegel et al. (1999). The “age” assumes that the supernova had a maximum on 1978 May 22 (MJD 43650).

The curves in Figure 2 are the best fits to the first 8 epochs of radio observation (Schlegel et al. 1999) using a modified version of the Weiler, Panagia, & Sramek (1990)

model for the evolution of Type II supernovae described in Montes, Weiler, & Panagia (1997). Figure 2 shows that while the evolution has generally continued to follow the model curves, there have been significant deviations from a smooth decay. In particular, there was a major dip at higher frequencies in April 2002. The most recent observation suggests a return to the long term rate of decline at each frequency.

2.3. Radio Implications

The most recent radio observations of SN 1978K show that it continues to be easily detectable more than a quarter of a century after the explosion, but with increasing deviations from a smooth decline.

The first tentative VLBI detection of a resolved remnant ~ 10 mas in size would correspond to a diameter of 0.2 pc, which allows us to place an upper limit on the average expansion velocity of 4000 km s^{-1} .

The significant departures from a smooth decline likely reflect changes in the circumstellar medium density. This indicates that a major change occurred in the mass-loss rate of the progenitor star prior to the supernova event. The time that this change took place depends on the assumed stellar wind velocity, and thus the progenitor type. For a Wolf-Rayet/LBV progenitor with a stellar wind $\sim 2000 \text{ km s}^{-1}$, the change in mass-loss rate must have occurred $\sim 4000/2000 \times 25 = 50$ years before the explosion. For a red supergiant wind speed of $\sim 20 \text{ km s}^{-1}$ the change would have occurred 5,000 years earlier.

Chugai, Danziger, & Della Valle (1995) suggested that variations in the $\text{H}\alpha$ luminosity were similarly due to a clumpy circumstellar material. Assuming a wind speed of $\sim 10 \text{ km s}^{-1}$, they inferred that this could be explained by changes in the mass-loss $3,000 - 10,000$ years prior to the explosion.

3. X-ray Observations

NGC 1313 is close enough that *XMM-Newton* can simultaneously perform detailed spectroscopic and timing studies of all the ULXs in short observations.

3.1. *XMM-Newton* Observations

In *XMM-Newton* Cycles 2 and 3, we performed a series of ~ 10 ksec Priority A observations to investigate the evolution of the ULXs and the other X-ray sources in NGC 1313 on a variety of time scales.

In Cycle 2, eight observations took place between 2003-11-25 and 2004-01-16. Unfortunately, several of these were affected by soft proton flaring that limit their usefulness for detailed analysis. In Cycle 3, we observed approximately every three months (the first observation was redone due to a slew failure) to monitor the longer-term variability.

All the Cycle 2 and 3 observations were centered on ULX X-2. An advantage of using *XMM-Newton* to observe NGC 1313 is that ULX X-1, X-2, and SN 1978K are all well within the field of view in a single pointing. However, depending on the satellite orientation, in some of the observations SN 1978K was located on or very close to a bad column in one of the detectors, or on or near a boundary between MOS or pn CCDs: in these cases, little or no useful data was collected by one or more of the detectors.

The *XMM-Newton* observation on 2003-12-09 was fully simultaneous with a portion of the ATCA observation. Unfortunately, this *XMM-Newton* observation was plagued by flares, and none of the data taken that day are useful. The *XMM-Newton* observation on 2004-11-23 was fully simultaneous with a portion of the ATCA observation. The whole of this *XMM-Newton* observation was unaffected by flares. However, a dark column ran through SN 1978K in the pn data, and thus only the MOS1 and MOS2 data are useful for that day.

In Table 2 we list all our *XMM-Newton* observations from Cycles 2 and 3. We have also re-analyzed the observation of NGC 1313 from 2000-10-17 (PI: Bernd Aschenbach). For each observation, we list the detectors that were used in the modeling of SN 1978K in §3.2, and the cleaned exposure times. While some of these spectra have short exposure times due to the flaring, leaving out the poorest spectra does not make any significant difference to the fitting results.

All the 2003-2005 observations were made in Full Frame EPIC mode, and used the thin optical blocking filter. Although the sources in NGC 1313 are bright, pile-up was not a problem for any of them. The total count rate limits for the detectors were not reached thanks to the low diffuse emission from the galaxy.

All the 2000-2005 data were reduced using version 6.5 of the *XMM-Newton* Science Analysis System (SAS). A couple of test cases were re-reduced using the newer version 7.0 of SAS, but this did not result in any significant changes. The spectral and timing analysis was performed using HEASoft version 6.1.

The data reduction followed the standard steps in SAS. For all the data, the pipeline processing was redone using `emchain` and `epchain`. The times were determined when soft proton flaring was significant – when the full-image count rate for photons > 10 keV was above 0.35 cps for the MOS and above 1 cps for the pn – and these data segments were removed. Images were made for each detector, and it was examined whether SN 1978K was significantly affected by bad columns on the CCD or by the boundary between CCDs. There were no Out of Time problems for the source. Spectra and light curves were made for SN 1978K using the 0-12 X-ray patterns for the MOS and the 0-4 patterns for the pn. A $40''$ extraction radius around the source was used. The data were screened for defects with `#XMMEA_EM` (MOS) or `#XMMEA_EP` (pn), and events next to the CCD edges were excluded using `FLAG=0`. Background spectra and light curves were made in the same fashion using a nearby region on the same CCD that was free of defects. Since the telescope orientation was not the same for each observation, the location of the background region changed with time; however, this was not a significant problem since the background flux was always much lower than that of the source. Photon redistribution matrices (RMF) and ancillary region files (ARF) were generated for the location of SN 1978K for use in the spectral analysis. The calibration of the EPIC instruments was good enough that no fixed or floating normalization factors were needed to match the fluxes for the three detectors; the improved cross-calibration of the detectors in SAS 6.5 fixed the problems in our initial analysis (Stacy 2005).

After our original manuscript was submitted, an additional *XMM-Newton* observation of NGC 1313 taken on 2006-03-06 became publicly available (PI: Stefan Immler). This observation was long and clean – with very little soft proton flaring – and was centered on SN 1978K. The medium optical blocking filter was used in this observation. The 2006-03-06 data were reduced with SAS 7.0 in the same manner as the other data. We found that the 2006-03-06 observation is well fit by the model described in §3.2 that was used to fit the 2000-2005 data. Folding the 2006 data into the joint 2000-2005 fit leads to very small changes in the “best fit” values cited in §3.2; the optimized values are all well within the original errors for the parameters. Rather than re-writing all of §3.2, we have left that section as a discussion of the modeling of the 2000-2005 data. We have added §3.3 to discuss the fitting of the 2006 data, which acts as an independent test of the model.

3.2. Modeling 2000-2005 *XMM-Newton* Data

The X-ray emission from SN 1978K has been fit using an absorbed two-temperature optically thin hot thermal plasma model (dual `vmekal` in XSPEC) to model the forward

and reverse shocks formed by the interaction of the supernova ejecta with its surroundings (Schlegel et al. 2004).

Modeling the *XMM-Newton* spectra for each of the separate days, we find that acceptable statistical fits can be obtained using a range of model parameters. Since fluctuations in the X-ray light curve with amplitudes $\sim 20\%$ might be seen if the ejecta are significantly inhomogeneous (or more based on the radio variability), we do not necessarily expect to get the same fit results for each day. It is also plausible that the X-ray light curve might be decaying as a power law as the remnant expands (Schlegel et al. 1999), or it might brighten steadily if the supernova ejecta runs into a denser circumstellar envelope. There could also be other systematic variations – such as the temperatures cooling – in one or more of the parameters. However, since several of our observations span a relatively short range of time compared to the time since the explosion, significant changes in the model parameters may be less likely. Historically, the recent X-ray monitoring of SN 1978K has found it consistent with being constant (Schlegel et al. 2000).

To address the variability issue in a concrete way, we have combined all the *XMM-Newton* data from 2000 to 2005 and investigated whether there is a model that can simultaneously fit all this data. This assumes that there is no systematic evolution or significant short-term variability for any of the fit parameters. If we were unable to find a good fit to the joint data, this would imply that one or more of the parameters was changing significantly. On the other hand, finding a good fit to the joint data does not necessarily guarantee that this is the correct result; the spectra from a variable source might by chance average out (although the increase in the number of photons in the joint fit makes this difficult to accomplish). Ultimately, as we illustrate in §3.3, the joint fit can be fully tested by using it to fit future observations, allowing for plausible slow long-term evolutions.

Our modeling of the combined data found that it was not possible to get a good fit using solar abundances for the hot plasmas. Assuming solar abundances for all the components, the best fit gives a reduced chi squared of $\chi^2_\nu = 1.26$ for $\nu = 1139$ degrees of freedom and an unacceptably low null hypothesis probability of $Q = 7.6 \times 10^{-9}$. This is shown in Figure 3. Although the temperatures of the vmekal components are similar to previous results (Schlegel et al. 2004), the value of $N_H = 1.16 \times 10^{21} \text{ cm}^{-2}$ in this case is rather low.

We investigated varying the abundances of the vmekal model components. We systematically tried allowing individual elements to vary without constraint (with the absorption, temperatures, and normalizations also unconstrained). We also tried allowing combinations of elements to vary without constraint. Surprisingly, we found that acceptable fits could only be attained in one special circumstance: the helium abundances in both the plasmas need to be large. This would imply that the X-ray emitting shocks are currently located in a

helium-rich layer that was ejected by the progenitor star, or helium-rich material was ejected in the supernova explosion. A representative fit is shown in Figure 4. The parameters for this fit are given in Table 3. With the exception of the helium abundances, the fit parameters are similar to those found previously by Schlegel et al. (2004). The fit has $\chi^2_\nu = 1.06$ for $\nu = 1137$ and $Q = 0.084$. The ratio of the model to the data does not have systematic variations, unlike the case when using solar abundances.

Fixing all the parameters of the large helium abundance model to the values given in Table 3, we compared the model to the data for each day separately to see if every day could be explained by the same model. Only one day gave an unacceptable result; 2004-05-01 had $Q = 1.8 \times 10^{-4}$. However, only MOS data was available for that day. For 2004-05-01, leaving all the parameters fixed at the values in Table 3 but allowing just the helium abundances to vary gave a good fit ($Q = 0.24$) with helium abundances of 7.5 for the hard component and 23.5 for the soft; these values are consistent with the original error bars for these parameters. The following observation on 2004-06-05 – that had more data – was well explained by the original fixed model ($Q = 0.44$). Thus if there was any deviation in the abundances, it was short-lived. The next worst day 2003-12-21 had $Q = 0.16$, which is a fine fit. Thus the individual day results are consistent with the assumption that there was no systematic evolution or large-scale variability.

For SN 1978K, the absorption found in our best joint fit is $N_H = (2.12^{+0.14}_{-0.16}) \times 10^{21} \text{ cm}^{-2}$. This is much higher than the value typically found for the rest of NGC 1313 plus the Milky Way ($N_H = 0.37 \times 10^{21} \text{ cm}^{-2}$). Thus this must be dominated by absorbing material close to SN 1978K. The value of N_H found in our joint fit is tightly constrained and agrees very well with the value of $N_H = (2.2 \pm 0.1) \times 10^{21} \text{ cm}^{-2}$ that was found from the mean H I column density measured around SN 1978K (Ryder et al. 1993). This adds further credence to our joint fit results and the large helium abundance model. The implication of our model is that the absorption is currently dominated by the material ejected by the supernova progenitor and/or its natal molecular cloud.

Schlegel et al. (2004) had a range of N_H in their different fits and suggested that N_H may be increasing with time. We instead conclude that N_H is consistent with remaining constant over the recent observations.

Schlegel et al. (2004) also suggested that an excess of silicon improved the fit. However, this only affects a couple of spectral bins and we do not find any significant improvements in the fit when the silicon abundances are varied.

We have studied varying the metallicity of the absorbing material for SN 1978K, but find no significant deviations from solar abundances. The fact that the absorption is currently

dominated by material close to the source means that the metallicity of the interstellar medium in NGC 1313 is not an important issue when fitting the SN 1978K X-ray spectra, unlike the case for the accreting ULXs. A low metallicity absorption is indicated when fitting the *XMM-Newton* data for the two accreting ULXs (Smith et al. 2004, 2007; Mizuno et al. 2007). This is consistent with other studies that have shown that the metallicity in NGC 1313 is a factor of 4 lower than in the Milky Way and that this is the highest mass barred spiral without a radial abundance gradient (Walsh & Roy 1997; Mollá & Roy 1999). Allowing for a low abundance of oxygen is particularly important when modeling the low temperature soft component in ULXs which has been interpreted as being disk blackbody emission from an optically thick disk around a $\sim 1000 M_{\odot}$ black hole.

The unabsorbed fluxes from SN 1978K in the 0.5 – 2 keV and 2 – 10 keV bands are 7.6×10^{-13} ergs cm $^{-2}$ s $^{-1}$ and 3.2×10^{-13} ergs cm $^{-2}$ s $^{-1}$ respectively. These fluxes are similar to those in Schlegel et al. (2004). Assuming a distance of 4.13 Mpc (Méndez et al. 2002), the corresponding luminosities are 1.6×10^{39} ergs s $^{-1}$ (0.5 – 2 keV) and 6.5×10^{38} ergs s $^{-1}$ (2 – 10 keV). The luminosity for the whole 0.2 – 10 keV band is 2.9×10^{39} ergs s $^{-1}$.

3.3. Testing the Model using the 2006 *XMM-Newton* Data

The long clean 2006-03-06 *XMM-Newton* observation of SN 1978K was used as an independent test of the results found in §3.2.

As was found when fitting the 2000-2005 data, the 2006-03-06 data cannot be fit using a dual vmekal model with solar abundances for the hot plasmas. The best fit in this case gives $\chi^2_{\nu} = 1.42$ for $\nu = 283$ and an unacceptably low $Q = 4.7 \times 10^{-6}$.

The 2006-03-06 observation is well fit by the large helium abundance model described in §3.2 that fit the 2000-2005 data. Using the parameters from Table 3 – with no additional optimization – the fit has $\chi^2_{\nu} = 1.09$ for $\nu = 281$ and $Q = 0.14$.

Folding the 2006 data into the joint 2000-2005 fit leads to very small changes in the “best fit” values for the large helium abundance model given in Table 3. The new values are all well within the original errors for the parameters.

These results bolster the conclusions that (1) there has been no significant evolution of the X-ray parameters recently, and (2) the large helium abundance model gives a good explanation for the 2000-2006 data.

4. Search for an Associated Gamma-Ray Burst

In models for long-duration GRBs, it is thought that the progenitor star at least ejects its hydrogen envelope prior to the supernova/hypernova (e.g. Woosley & Heger 2006). If this did not take place, the relativistic jet would not escape with sufficient energy to make a long GRB. However, only a tiny fraction of massive stars produce a GRB when they die, perhaps $\sim 1\%$ (Guetta & Della Valle 2007). This leads to the question of what features of the progenitor are necessary/sufficient to produce a GRB. Although GRBs are believed to be associated with Type Ib or Ic supernovae, given the rare and unusual nature of the Type IIn SN 1978K and the fact that it had significant ejections prior to the explosion, we have searched for any GRBs that might have been associated with this supernova.

Based on the optical observations summarized in §1, the supernova explosion took place some time between 1977 October 12 and 1978 July 31. These dates bracket our search for an associated GRB. The Interplanetary Network (IPN) of GRB satellites has existed since 1976. Several GRB detectors were operational during the window for SN 1978K. However, the first wide-baseline three-cornered network did not exist until the launch of the Veneras in 1978 September (Atteia et al. 1987). Thus the localization of the bursts was poor during the SN 1978K window.

Klebesadel et al. (1982) used the data from the available satellites to determine the GRBs that were detected by at least two instruments on separate satellites. Other events may have been real bursts, but only the confirmed GRBs were reported. In the SN 1978K window, 6 confirmed GRBs were detected: GRB 771020, GRB 771029, GRB 771110, GRB 780508, GRB 780519, and GRB 780521.

Based on the locations of these bursts (Klebesadel et al. 1982), 5 of them are clearly not consistent with the location of SN 1978K. However, GRB 771029 is close to SN 1978K; the supernova is inside the $\sim 4\sigma$ error box of GRB 771029. Unfortunately, the uncertainty in the location for this burst is large, and the probability that SN 1978K would lie in the 4σ error annulus is 14%. Thus this may be just a chance alignment.

GRB 771029 was a long-duration burst, lasting ~ 15 sec (Éstulin et al. 1978). It was detected in the 140 – 300 keV band by SIGNE 2MP detector S on Prognosz 6. GRB 771029 emitted $< 10^{-5}$ erg cm $^{-2}$ and so was less energetic than the other two Prognosz 6 events ($> 2 \times 10^{-5}$ erg cm $^{-2}$). Assuming an isotropic gamma-ray emission and a distance of 4.13 Mpc, the burst energy would have been $< 2 \times 10^{46}$ ergs. There are currently 3 examples of highly underluminous long-duration GRBs associated with relatively nearby supernovae (Cobb et al. 2006). The least luminous was GRB 980425/SN 1998bw that had an isotropic gamma-ray energy of $\sim 10^{48}$ ergs. Thus if GRB 771029 was associated with SN 1978K, this

would have been an exceptionally underluminous burst. However, we do not know what luminosity should be expected for a GRB associated with a Type IIn supernova.

An argument against the association of GRB 771029 and SN 1978K is that the radio and optical emissions likely peaked in 1978 May, which would be many months after the burst. The existence of lags between the GRB and supernova events is not currently supported by observations. For example, in the GRB 060218/SN 2006aj association (Campana et al. 2006), the supernova and GRB were coeval to within $\lesssim 1$ day.

5. Conclusions

The rare Type IIn supernova SN 1978K remains bright in radio and X-rays ~ 25 years after the explosion. The $0.2 - 10$ keV luminosity is 2.9×10^{39} ergs s $^{-1}$.

The radio imaging shows that the source remains compact, but it may be marginally resolved, ~ 10 mas in size corresponding to a diameter of 0.2 pc. The recent radio observations show deviations from a smooth decay suggesting that inhomogeneities are present in the radio emitting region. It appears that a major change occurred in the mass-loss rate of the progenitor star – possibly a LBV – shortly before the supernova event.

The winds from the progenitor star produced a dense medium. The X-ray emission is consistent with coming from two shocks in this medium. The *XMM-Newton* observations from 2000 to 2006 can all be fit using the same model, with no systematic evolution or short-term variability. While the model parameters that we find are similar to those in previous studies, the new element of our modeling is the large abundance of helium. This suggests that the shocks are located in a helium-rich layer that was ejected by the progenitor star, or helium-rich material was ejected in the supernova explosion.

Using the large helium abundance model, the value of N_{H} is tightly constrained and agrees very well with the value found from the mean H I column density measured around SN 1978K. This indicates that the absorption is currently dominated by the material ejected by the progenitor and/or its natal molecular cloud. The value of N_{H} is consistent with remaining constant over the recent observations.

The unusual properties of the supernova motivated a search for an associated GRB. Considering just the confirmed GRBs, only one GRB is consistent with the location of SN 1978K; the supernova is inside the $\sim 4\sigma$ error box of GRB 771029. However, this is likely just a chance alignment.

It is of particular interest to continue to study the long-term multiwavelength evolution

of this rare supernova to study the mass-loss history of the progenitor star. By continuing to watch how SN 1978K evolves, it will be possible to understand whether the unusually dense circumstellar medium is the result of an extreme mass-loss rate, a low wind velocity, or the presence of cavities and clumps. Is the mass loss at late epochs episodic (resulting in an onion-like shell structure)? Is it bipolar, with rings and hotspots as in SN 1987A? Is there evidence that a GRB took place, even if the burst was not beamed towards Earth? Ultimately, is it the environment or intrinsic factors that dictates which stars end their lives as Type II_n supernovae? While it is expected that there will be a slow evolution (\sim years) of the plasma temperatures, normalizations, and/or abundances, the variability of the radio indicates that changes on shorter time scales should continue to be investigated.

This work has been supported by NASA grants NNG04GC64G and NNG04G100G at Rice University and NNG04GC65G and NNG04GI50G at Ohio University.

The Australia Telescope Compact Array and Australian Long Baseline Array are part of the Australia Telescope which is funded by the Commonwealth of Australia for operation as a National Facility managed by CSIRO.

XMM-Newton is an ESA science mission with instruments and contributions directly funded by ESA Member States and NASA.

We thank the referee for helpful comments.

Facilities: ATCA, Hobart, Mopra, Parkes, Tidbinbilla, XMM.

REFERENCES

- Atteia, J.-L., et al. 1987, ApJS, 64, 305
- Bregman, J. N., Houck, J. C., Chevalier, R. A., & Roberts, M. S. 2003, ApJ, 596, 323
- Campana, S., et al. 2006, Nature, 442, 1008
- Cannon, W. M. et al. 1997, Vistas Astron., 41, 297
- Chu, Y.-H, Caulet, A., Montes, M. J., Panagia, N., Van Dyk, S. D., & Weiler, K. W. 1999, ApJ, 512, L51
- Chugai, N. N., Danziger, I. J., & Della Valle, M. 1995, MNRAS, 276, 530
- Cobb, B. E., Bailyn, C. D., van Dokkum, P. G., & Natarajan, P. 2006, ApJ, 645, L113

- Colbert, E. J. M., & Mushotzky, R. F. 1999, *ApJ*, 519, 89
- Colbert, E. J. M., Petre, R., Schlegel, E. M. & Ryder, S. D. 1995, *ApJ*, 446, 177
- Éstulin, I. V., Kuznetsov, A. V., Vedrenne, G., Niel, M., & Hurley, K. 1978, *Sov. Ast. Lett.*, 4, 239
- Fabbiano, G., & Trinchieri, G. 1987, *ApJ*, 315, 46
- Feng, H., & Kaaret, P. 2007, *ApJ*, 660, L113
- Gruendl, R. A., Chu, Y.-H., Van Dyk, S. D., & Stockdale, C. J. 2002, *AJ*, 123, 2847
- Guetta, D., & Della Valle, M. 2007, *ApJ*, 657, L73
- Klebesadel, R., et al. 1982, *ApJ*, 259, L51
- Larsen, S. S. 1999, *A&AS*, 139, 393
- Liu, J., Bregman, J., Miller, J., & Kaaret, P. 2007, *ApJ*, 661, 165
- Méndez, B., Davis, M., Moustakas, J., Newman, J., Madore, B. F., & Freedman, W. L. 2002, *AJ*, 124, 213
- Miller, J. M., Fabbiano, G., Miller, M. C., & Fabian, A. C. 2003, *ApJ*, 585, L37
- Miller, J. M., Fabian, A. C., & Miller, M. C. 2004, *ApJ*, 607, 931
- Miller, S., Schlegel, E. M., Petre, R., & Colbert, E. 1998, *AJ*, 116, 1657
- Mizuno, T., et al. 2007, *PASJ*, 59, S257
- Mollá, M., & Roy, J.-R. 1999, *ApJ*, 514, 781
- Montes, M. J., Weiler, K. W., & Panagia, N. 1997, *ApJ*, 488, 792
- Mucciarelli, P., Zampieri, L., Treves, A., Turolla, R., & Falomo, R. 2007, *ApJ*, 658, 999
- Pakull, M. W., & Mirioni, L. 2002, *New Visions of the X-ray Universe in the XMM-Newton and Chandra Era*, astro-ph/0202488
- Pakull, M. W., & Mirioni, L. 2003, *RevMexAA*, 15, 197
- Pakull, M. W., Gris , F., & Motch, C. 2006, *Populations of High Energy Sources in Galaxies, Proceedings of the 230th Symposium of the IAU*, E. J. A. Meurs & G. Fabbiano, Cambridge: Cambridge University Press, 293

- Ryder, S., Staveley-Smith, L., Dopita, M., Petre, R., Colbert, E., Malin, D., & Schlegel, E. 1993, *ApJ*, 416, 167
- Ryder, S. D., Staveley-Smith, L., Malin, D., & Walsh, W. 1995, *AJ*, 109, 1592
- Schlegel, E. M., Petre, R., & Colbert, E. J. M. 1996, *ApJ*, 456, 187
- Schlegel, E. M., Ryder, S., Staveley-Smith, L., Petre, R., Colbert, E., Dopita, M., & Campbell-Wilson, D. 1999, *AJ*, 118, 2689
- Schlegel, E. M., Petre, R., Colbert, E. J. M., & Miller, S. 2000, *AJ*, 120, 2373
- Schlegel, E. M., Kong, A., Kaaret, P., DiStefano, R., & Murray, S. 2004, *ApJ*, 603, 644
- Shepherd, M. C., Pearson, T. J., & Taylor, G. B. 1994, *BAAS*, 26, 987
- Smith, I. A., Böttcher, M., Ryder, S., & Pakull, M. W. 2004, *BAAS*, 36 #3, 15.16
- Smith, I. A., Böttcher, M., Pakull, M. W., Ryder, S., & Stacy, A. 2007, *ApJ*, in preparation
- Stacy, A. 2005, Senior Thesis, Rice University
- Stocke, J. T., Wang, Q. D., Perlman, E. S., Donahue, M. E., & Schachter, J. F. 1995, *AJ*, 109, 1199
- Walsh, J. R., & Roy, J.-R. 1997, *MNRAS*, 288, 726
- Weiler, K. W., Panagia, N., Sramek, R. A. 1990, *ApJ*, 364, 611
- Wilson, W. E., Davis, E. R., Loone, D. G., & Brown, D. R. 1992, *J. Electrical Electron. Eng. Australia*, 12, 187
- Woosley, S. E., & Heger, A. 2006, *ApJ*, 637, 914
- Zampieri, L., Mucciarelli, P., Falomo, R., Kaaret, P., Di Stefano, R., Turolla, R., Chierigato, M., & Treves, A. 2004, *ApJ*, 603, 523

Table 1. ATCA radio observations of SN 1978K

UT Date	MJD	Age (days)	Flux Densities (mJy)			
			1376 MHz	2496 MHz	4790 MHz	8640 MHz
2000-01-04	51547	7897	78.3 ± 1.0	50.7 ± 1.0	31.8 ± 0.9	18.2 ± 1.7
2000-05-25	51689	8039	72.8 ± 1.4	50.4 ± 0.5	32.9 ± 2.5	18.9 ± 2.0
2000-09-10	51797	8147	73.4 ± 0.7	49.6 ± 0.4	32.3 ± 0.5	20.5 ± 0.4
2001-02-07	51948	8298	71.0 ± 0.5	46.8 ± 0.4	29.3 ± 0.4	16.6 ± 0.5
2002-04-09	52374	8724	62.9 ± 1.5	43.2 ± 0.4	25.6 ± 0.4	12.5 ± 0.7
2003-12-09	52983	9333	55.7 ± 1.0	38.9 ± 0.5	25.5 ± 0.6	14.9 ± 0.6
2004-11-23	53333	9683	49.5 ± 2.3	37.1 ± 0.5	24.6 ± 0.5	15.3 ± 0.4

Table 2. *XMM-Newton* observations of SN 1978K

Start Date (UT)	Observation ID	Detectors with good data	Exposure times (ksec)
2000-10-17	0106860101	MOS2, pn	26.1, 20.2
2003-11-25	0150280101	MOS1, MOS2	2.5, 2.5
2003-12-09	0150280201	none	
2003-12-21	0150280301	MOS1, MOS2, pn	10.2, 10.3, 7.6
2003-12-23	0150280401	MOS1, MOS2	6.2, 6.8
2003-12-25	0150280501	MOS1	8.4
2003-12-27	0150280701	none	
2004-01-08	0150280601	MOS1, MOS2, pn	12.7, 13.0, 7.1
2004-01-16	0150281101	MOS1, MOS2	7.8, 7.7
2004-05-01	0205230201	MOS1, MOS2	7.8, 8.0
2004-06-05	0205230301	MOS1, MOS2, pn	11.5, 11.5, 8.9
2004-08-23	0205230401	MOS1, MOS2, pn	13.1, 13.9, 4.4
2004-11-23	0205230501	MOS1, MOS2	15.5, 15.5
2005-02-07	0205230601	MOS1, MOS2, pn	12.2, 12.4, 8.5
2006-03-06	0301860101	MOS1, MOS2, pn	21.3, 21.3, 17.5

Table 3. Parameters used in the absorbed dual vmekal modeling of the joint fit to the 2000-2005 *XMM-Newton* observations of SN 1978K. All the other abundance parameters are set to 1.0. Each error gives an estimate of the 90% confidence region for a single interesting parameter.

Model component	Parameter	Best fit
vphabs	$N_{\text{H}} (\times 10^{21} \text{ cm}^{-2})$	$2.12^{+0.14}_{-0.16}$
soft vmekal	kT (keV)	$0.61^{+0.02}_{-0.02}$
	He	$39.2^{+9.5}_{-9.2}$
	Norm ($\times 10^{-4}$)	$0.92^{+0.06}_{-0.05}$
hard vmekal	kT (keV)	$3.37^{+0.50}_{-0.42}$
	He	$8.9^{+9.2}_{-2.8}$
	Norm ($\times 10^{-4}$)	$1.36^{+0.38}_{-0.61}$

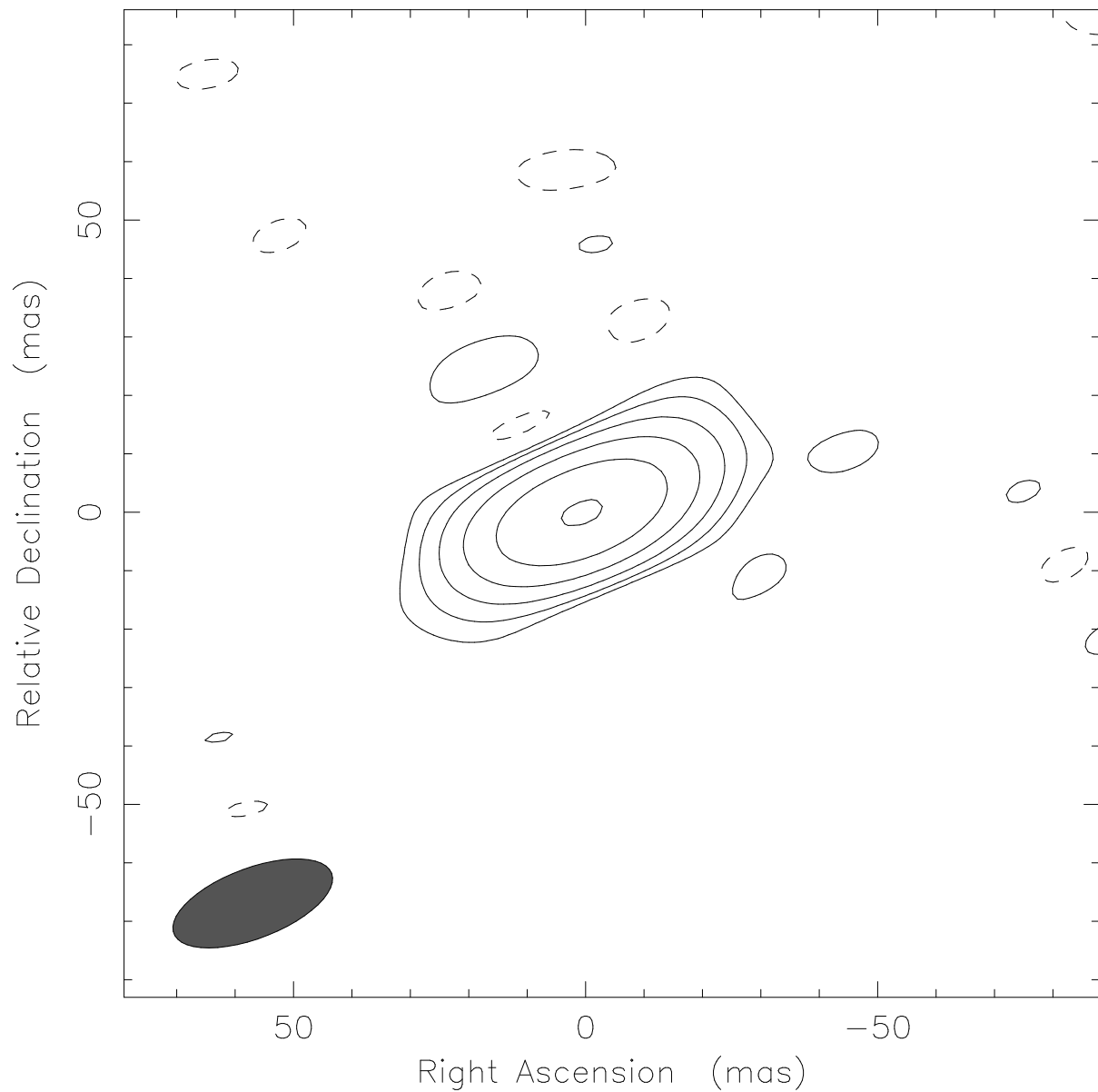


Fig. 1.— VLBI image of SN 1978K at a frequency of 2.3 GHz on 2003 March 22. The map is centered at 03:17:38.62, $-66:33:03.4$ (J2000). The peak flux density in the image is 28 mJy/beam and the rms image noise is 0.5 mJy/beam. The beam is $29\text{ mas} \times 12\text{ mas}$ at a position angle of -69° . Contours are shown at $\pm 3\%$, 6%, 12%, 24%, 48%, and 96% of the peak flux density.

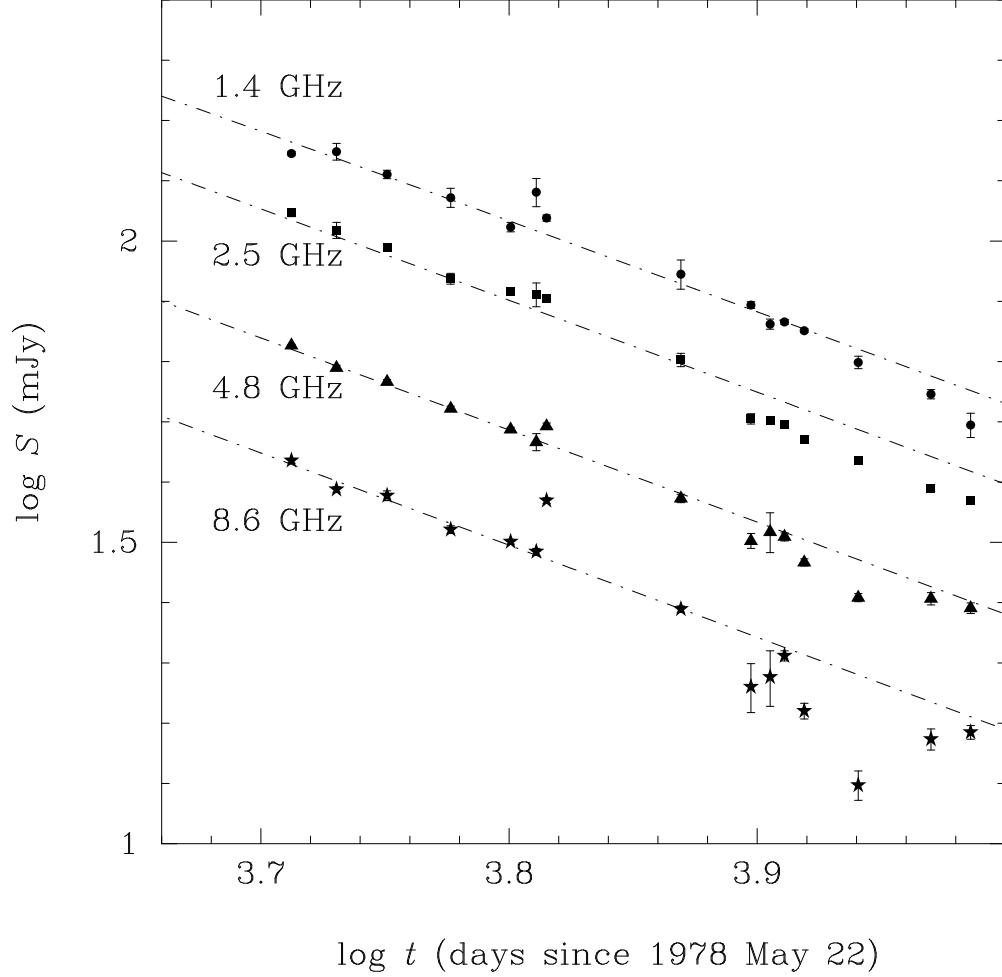


Fig. 2.— The radio light curves for SN 1978K from ATCA monitoring between 1991 and 2004. This adds seven points to each of the curves shown in Schlegel et al. (1999). The curves are the best fits to the first 8 epochs of radio observation using a modified version of the Weiler, Panagia, & Sramek (1990) model for the evolution of Type II supernovae described in Montes, Weiler, & Panagia (1997).

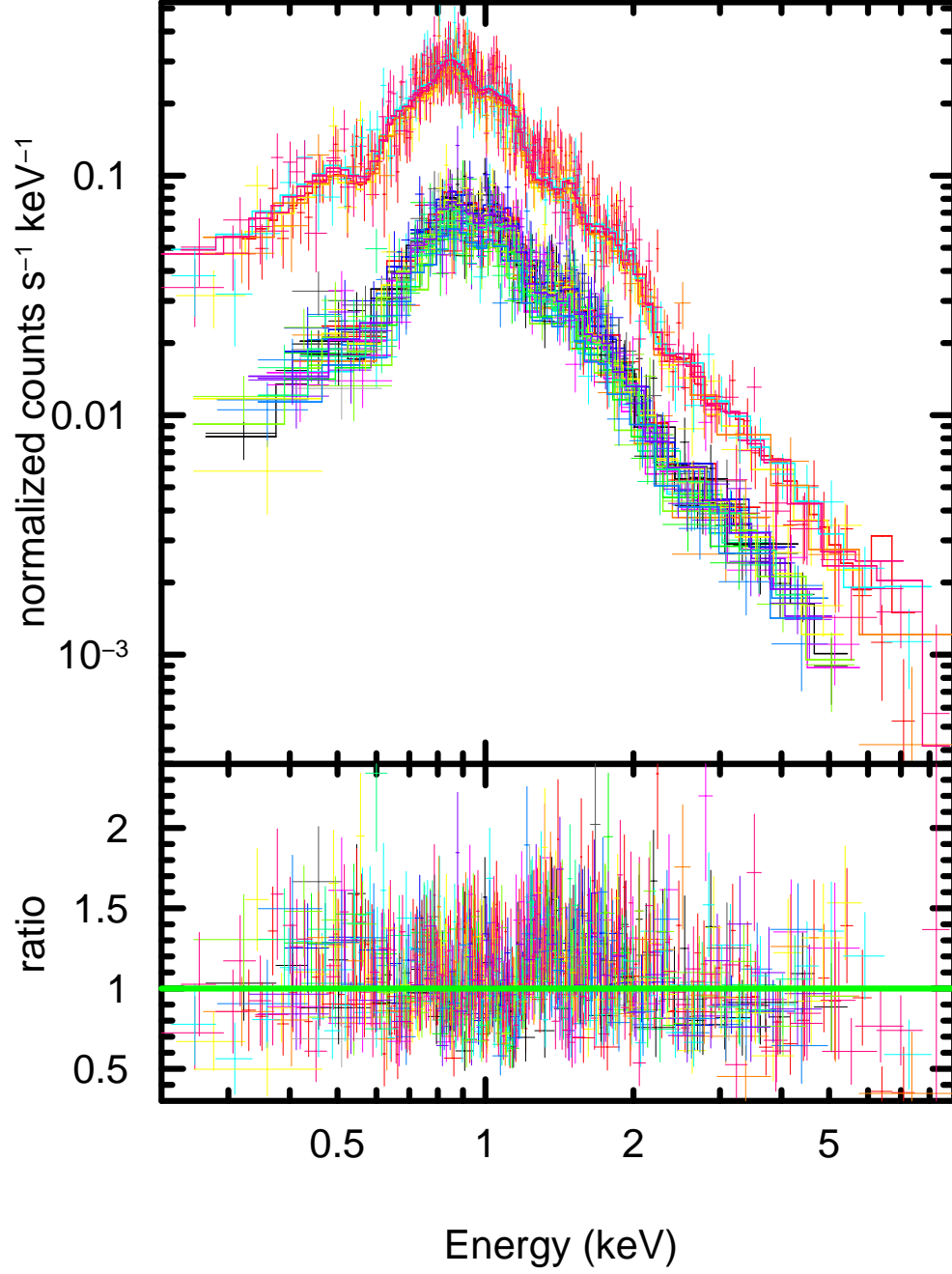


Fig. 3.— Fit to all the *XMM-Newton* observations of SN 1978K from 2000 through 2005 using an absorbed dual vmekal model with solar abundances in the hot plasmas. See the electronic edition of the Journal for a color version of this figure.

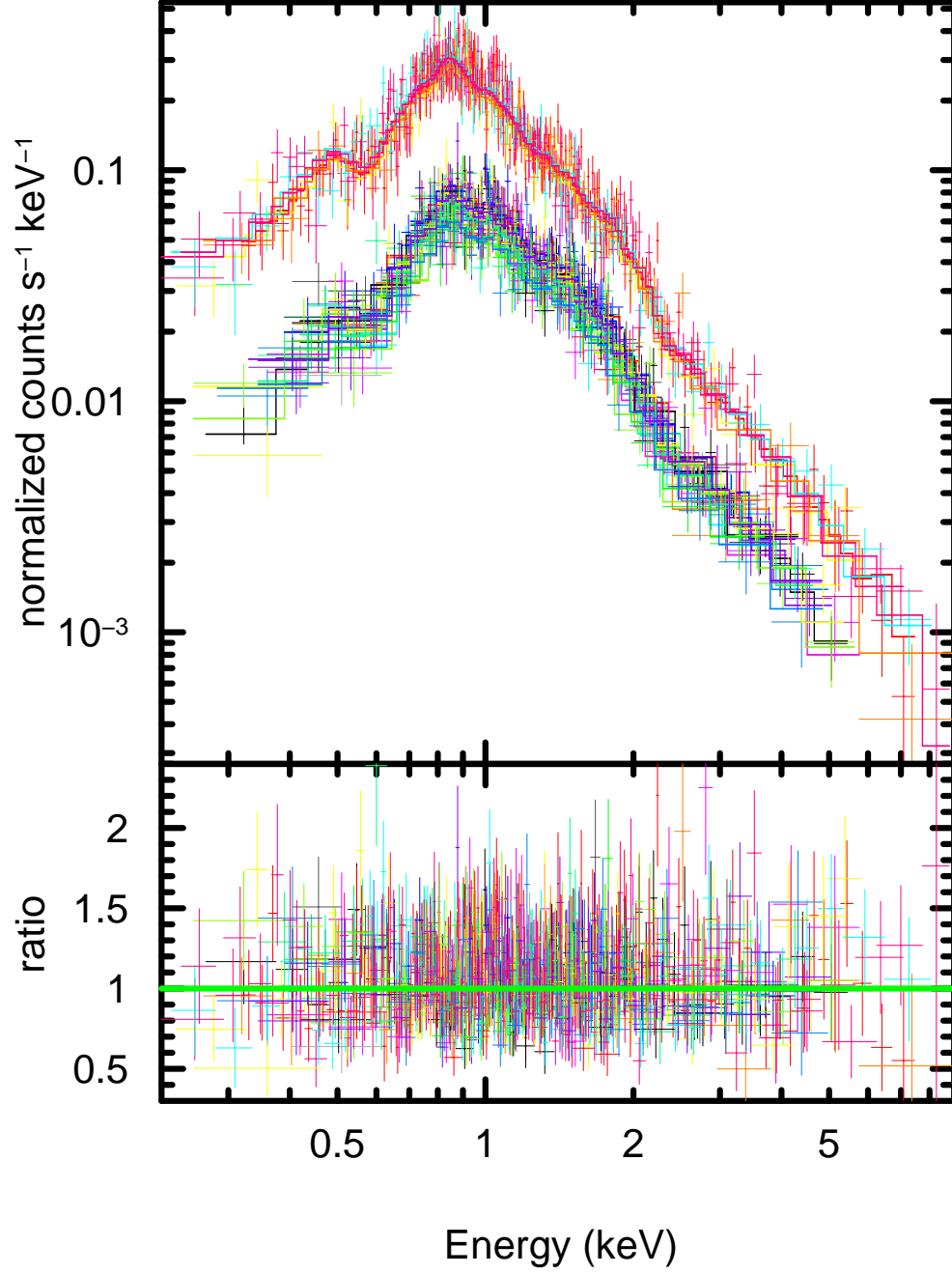


Fig. 4.— Fit to all the *XMM-Newton* observations of SN 1978K from 2000 through 2005 using an absorbed dual vmekal model with large helium abundances in the hot plasmas. See the electronic edition of the Journal for a color version of this figure.